AADE-20-FTCE-031

Absorption Kinetics of Gas Influxes into Nonaqueous Fluids During Riser Gas Handling Events

Scott Perry, Chen Wei and Yuanhang Chen, Louisiana State University

Abstract

The absorption kinetics of an influx of hydrocarbon gas into a nonaqueous base fluid was experimentally investigated under various conditions. The gas influx was simulated by continuously injecting methane at different pressures and superficial gas velocities into an experimental column filled with nonaqueous base fluids. The concentration of gas dissolved into the base fluids was measured at various time steps until complete saturation was reached. A model containing an absorption coefficient, $k_L a$, was used to describe the process. The time dependent absorption mass transfer coefficient can be determined for each set of experimental conditions to develop a relationship between $k_L a$ and the input parameters. The effects of pressure, superficial gas velocity and base fluid on the mass transfer absorption coefficient were examined in the study. The impact of the time-dependent gas absorption process on gas migration behaviors during a riser gas handling event, were simulated using a simplified two-phase model along with a kinetic mass transfer sub-model based on the experimental study performed in this work. The results of this experimental study and numerical simulations provide better understanding of time dependent absorption of gas influx into uncontaminated muds while migrating and its effects on unloading behaviors with different backpressures, and therefore can be used to optimize and guide operations in such events.

Introduction

When the hydrostatic pressure of the drilling fluid drops below the formation pressure, an influx of natural gas trapped in the pores can enter the wellbore (Neff et al. 2000). When using aqueous drilling fluids, the natural gas will stay in the gaseous phase without dissolving into the fluid as it travels to the surface. On the other hand, when drilling with non-aqueous drilling fluids, severe problems can arise as the gas kick has the potential to be absorbed into the drilling fluids. The reason that these problems arise is due to the gas's potential to be hidden due to gas absorption. There will be little to no absorption while using water based drilling fluids that will generate a large pit gain at the surface (O'bryan 1983). At high bottom-hole pressures in the wellbore, a large volume of hydrocarbon gas can be absorbed into nonaqueous-based drilling fluids and go undetected as the drilling fluid is circulated up the wellbore. As the dissolved gas is circulated up the wellbore, severe problems can occur once gas desorbs from solution and expands rapidly as the wellbore pressure decreases.

A unique scenario of gas absorption and one that is becoming important to well control operations is when dissolved or free gas passes the subsea blowout preventer (SSBOP), enters the riser and begins to evolve from solution. As free gas migrates to the surface, the free gas will be absorbed into the uncontaminated drilling mud due to the slippage between the gas and liquid phase during riser gas handling. With new drilling techniques and technology, like managed pressure drilling (MPD), riser gas migration can be better controlled and managed because of their ability to quickly change the equivalent circulating density (ECD) of the fluid within the well. During MPD, a choke can be used at the surface to adjust the flow rate of drilling fluid and subsequently increase the pressure within the riser. Once the pressure is increased using the MPD choke or a backpressure pump, the expansion of free gas that has desorbed from the drilling fluid could potentially dissolve back into solution (Malloy et al. 2009). It is important to understand the behavior of gas with changing pressure and superficial gas velocity on different types of drilling fluids to control and prevent significant problems during well control in such events.

Gas Absorption Mass Transfer

Gas absorption is a process that requires mass transfer of soluble components from the gas stream to the liquid phase when the gas flows through the liquid (Elhajj et al. 2013). Due to greater solubility of gas in oil-based muds, an influx of gas can easily be absorbed into the drilling fluid and go undetected at the surface. Better understanding the absorption kinetics during a gas influx will help with earlier kick detection and prevent the influx from going undetected. To better understand this mass transfer between the influx of natural gas and non-aqueous drilling fluid, experimental tests were conducted to

determine the absorption mass transfer coefficient ($k_L a$). For mass transfer, it is expected that the amount transferred is proportional to the concentration difference and the interfacial area. Because the interfacial area between the gas and liquid face is unknown during an absorption experiment, the product of the mass transfer coefficient and area is experimentally determined together. Current industrial software assumes instantaneous gas absorption when an influx of gas enters the well at elevated pressure conditions. Because this can poorly represent absorption and gas migration, it is critical to more thoroughly understand mass transfer of gas influxes in oil-based fluids.

Most of the previous literature that exists on absorption mass transfer coefficients are experiments that were conducted with CO_2 and water. Investigations into the mass transfer of CO_2 into water have been conducted for nearly a century and relied on models focusing on applications of Henry's Law. In all absorption studies, investigations relied on injecting gas using a bubble column and then using a carrier gas to remove the absorbed gas through a gas stripping process before measuring the absorbed gas. Authors studying mass transfer kinetics have stated that the absorption and desorption mass transfer coefficients are equivalent, but only the absorption $k_L a$ value are determined in these experiments. Numerous experiments have been carried out in bubble column reactors to determine $k_L a$ values and several empirical correlations were proposed in gas-liquid systems (Ghandi et al. 2009)

According to Ghandi et al. (2009) there are several key factors that can affect the absorption mass transfer coefficient. Due to limitations in the bubble column, the factors experimentally tested to observe the effect on $k_L a$ were the pressure, superficial gas velocity and fluid type within the system. Table 1 shows all the key parameters affecting gas-liquid mass transfer, but only 3 of the 13 parameters provided by Ghandi et al. (2009) will be investigating in this experimental study. Once the effect on the mass transfer coefficient from these 3 parameters are evaluated and determined, the bubble column can be improved to test factors such as bubble size (using different sparger types), temperature of the system, column diameter and different liquid and gas physical properties.

Table 1: Parameters affecting absorption coefficient

Key Parameters Affecting Absorption Mass Transfer Coefficient	
Column Dimensions	Diameter Height
Sparger Type	Hole Diameter (Bubble Diameter) Number of Holes
System Properties	Temperature Pressure
Superficial Velocity	Gas Liquid
Liquid Properties	Density Viscosity Surface Tension
Gas Properties	Density Viscosity

In a gas-liquid mass transfer experimental study conducted by Lau et al. 2004, using oxygen and Paratherm Non-Fouling (NF) heat-transfer fluid, the effects of system pressure, gas and liquid velocities, column size and liquid properties on the mass transfer coefficient was investigated. As system pressure increases, bubble size decreases due to bubble breakup from higher gas density. As bubbles collapse, the bubble's size becomes smaller. The interfacial area will then increase between liquid and gas significantly resulting in an increase of $k_L a$ at higher pressures. $k_L a$ also increases with an increase in superficial gas velocity for similar reasons. At higher gas velocities, there is high gas holdup and an increase in turbulence furthermore resulting in an increased interfacial area. This increase in the interfacial area results in a higher $k_L a$ value even though there is a decrease in contact time between liquid and gas at high gas velocities. (Lau et al. 2004).

Lau et al (2004) proposed a correlation to predict $k_L a$ values for mass transfer between oxygen, water and Paratherm NF heat-transfer fluid. Equation 1 shows the empirical correlation proposed following the experimental investigation of several parameters on the mass transfer coefficient:

$$k_L a = 1.77\sigma^{-0.22} e^{1.65U_l - 65.3\mu_l} \epsilon_g^{1.2} \quad (1)$$

In the proposed correlation, the mass transfer coefficient can be calculated based on liquid surface tension, liquid velocity, liquid viscosity and gas holdup which has a significant impact on the interfacial area between liquid and gas. As this is a correlation for oxygen and water mass transfer, further investigation and experimental results would need to be generated to derive a correlation to accurately predict the $k_L a$ value for mass transfer between methane and non-aqueous fluids.

Ozturk et al. (1987) proposed the following correlation to determine the absorption mass transfer coefficient for the absorption of CO2 into an organic solution:

$$\frac{k_L a d_B^2}{D_L} = 0.62 \left(\frac{\mu_L}{\rho_L D_L}\right)^{0.5} \left(\frac{g\rho_L d_B^2}{\sigma_L}\right)^{0.33} \left(\frac{g\rho_L^2 d_B^3}{\mu_L^2}\right)^{0.29} \left(\frac{V_G}{\sqrt{g d_B}}\right)^{0.68} \left(\frac{\rho_G}{\rho_L}\right)^{0.04} \quad (2)$$

In this model, several factors including gas and liquid densities and bubble diameter were considered. In the experiments conducted, a sparger was used in the bubble column to effectively determine consistent bubble diameters and to know the exact number of bubbles in the column. To consider all 17 factors that could have a significant impact on the mass transfer coefficient, a complex model is needed to accurately represent the absorption phenomenon. Modeling the mass transfer of gas absorption becomes very complex when including all the parameters and factors that were considered in the Ozturk correlation.

Akita and Yoshida (1973) proposed the following model which takes into consideration gas holdup (ϵ_G) when calculating $k_L a$ from experiments of absorption of oxygen into

various liquids:

$$k_L a = \frac{1-\epsilon_G}{t} * ln\left(\frac{C^*-C_i}{C^*-C_f}\right) \quad (3)$$

A gas holdup correlation was determined from experimental data to calculate the mass transfer coefficient. The experimental data showed that gas holdup was a function of multiple parameters including column diameter, superficial gas velocity, kinematic viscosity and density of liquid, surface tension and gravity. The following equation shows the correlation between these parameters and the gas holdup term for oxygen into various liquids:

$$\frac{\epsilon_G}{(1-\epsilon_G)^4} = 0.2\left(\frac{g\rho_L}{\gamma}\right)^{0.125}\left(\frac{gD^3}{v_L^2}\right)^{0.833}\left(\frac{U_G}{\sqrt{gD}}\right) \quad (4)$$

Although gas holdup may influence the mass transfer coefficient, there is not a reliable method of measuring this term in our current experimental setup to determine its effects on the $k_L a$ for methane in non-aqueous drilling fluids. Alvarez et al. (2000) proposed a very similar model that also simplifies the problem by including several influencing parameters into an equation to measure the mass transfer coefficient as a function of time and the concentrations of gas in solution. This model allows for the calculation of $k_L a$ without accounting for gas holdup like in the previous model from Akita and Yoshida (1973). In the experimental setup, the effects of superficial gas velocity and physical properties of the absorbent liquid on the mass transfer coefficient were determined (Alvarez et at. 2000).

$$\frac{dC}{dt} = k_L a * (C^* - C) \quad (5)$$

$$\ln\left(\frac{C^*}{C^*-C_L}\right) = k_L a * t \quad (6)$$

$$k_L a = \frac{1}{t} * ln\left(\frac{C^*}{C^*-C_L}\right) \quad (7)$$

Equations 4-6 show the model proposed by Alvarez et al. (2000) in which experiments with CO_2 and an aqueous solution of sucrose and surfactants in a bubble column were performed to determine $k_L a$. Similarly, the same model used in the CO_2 experiment can be applied to describe mass transfer in absorption experiments with methane and non-aqueous drilling fluids.

Methodology

Experimental Design

With the current experimental apparatus, the 3 parameters in Table 2 were tested to determine the effects on the $k_L a$ using the following test matrix:

Table 2: Experimental Test Matrix

Test	*Pressure (psig)*	*Flow Rate (ln/min)*	*Corrected Flow Rate (L/min)*	*Superficial Gas Velocity (cm/s)*	*Base Fluid*
1	100	1.069	0.1369	0.45	Diesel
2	100	2.137	0.2738	0.90	Diesel
3	200	2	0.1369	0.45	Diesel
4	200	4	0.2738	0.90	Diesel
5	100	1.069	0.1369	0.45	IO
6	100	2.137	0.2738	0.90	IO
7	200	2	0.1369	0.45	IO
8	200	4	0.2738	0.90	IO

The effects that pressure, methane's superficial gas velocity, and the type of base fluid have on the absorption mass transfer coefficient are determined within the experimental scope of work of this paper. 8 experimental tests were conducted and parameters of each test are listed in Table 2. 100 and 200 psig to calculate the mass transfer coefficient at a pressure of 100 and 200 psi, superficial gas velocities of 0.448 and .895 cm/s and base fluid of diesel and internal olefins. Once the mass transfer coefficient was calculated for these 8 experiments, the effects of increasing the experimental pressure, gas velocity or changing base fluid type on the $k_L a$ value while holding the other factors constant could be determined.

Materials and Experimental Apparatus

Table 3 shows the experimental conditions and materials used during the investigation of the absorption coefficient for methane in nonaqueous fluids. The experimental apparatus shown in Figure 1, where methane was injected into the column filled with either diesel or internal olefin fluid. The experiments were performed at various operating pressures, superficial gas velocities and at an operaturing temperature of 295 K. The effects of the materials and experimental conditions on the $k_L a$ value were determined during this investigation.

Table 3: Experimental Conditions

Experimental Materials and Conditions	
Column Diameter	0.0254 m
Static Liquid Height	0.7112 m
Gas Phase	Pure Methane (CH_4)
Liquid Phase	Diesel Internal Olefins
Superficial Gas Velocity (U_g)	0.45 cm/s, 0.90 cm/s, 1.68 cm/s and 2.51 cm/s
Operating Pressure	100-200 psi
Operating Temperature	295 K

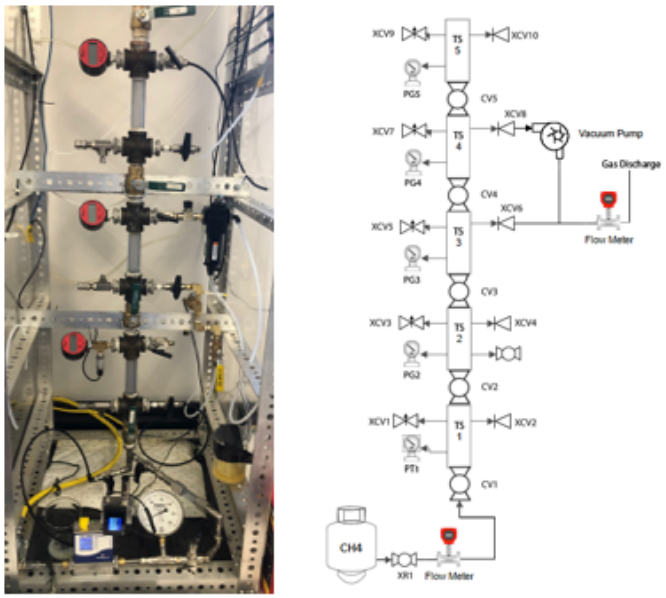

Figure 1: Low-pressure apparatus in the absorption configuration A) Picture of the experimental lab apparatus B) P&ID of the experimental lab apparatus

Experimental Procedure

Initially, the column in Figure 1 is empty and the vacuum pump is used to develop a vacuum within the experimental apparatus. Once a sufficient vacuum is generated, diesel or internal olefins are siphoned into TS1 and TS2 to fill both test sections completely. A nitrogen supply line connected at the top of the column is used to pressurize the column up to the desired experimental pressure (100 or 200 psi) before each test. Upon reaching the desired experimental pressure, the absorption experiment is ready to be conducted.

Using a regulator on the methane tank, the inlet at the bottom of TS1 is charged with methane to the same pressure as within the column before flowing methane through the fluid. The inlet and outlet valves are opened to allow the flow of methane through the diesel and absorption experiments are conducted for different durations of time from 30 seconds to 20 minutes. The inlet flow rate (1-6 ln/min) can be controlled using the outlet valves on the column. The totalized volume of gas influx and the flow rate is recorded on the inlet flow meter.

The methane flows through the test section for the designated amount of time before the amount of gas absorbed into the diesel is recorded. After each time interval, TS1 and TS2 that contain the fluid are isolated stopping the flow of gas through the column. While the TS1 and TS2 remained isolated, the vacuum pump is used on the column to remove any methane in the column to ensure the only measured methane flowing through the outlet flow meter is methane that was absorbed into the testing fluid. Once the column has a vacuum, the vacuum pump is used to pull the absorbed gas out of solution and through the outlet flow meter. The amount of gas that was absorbed in solution at each time interval is recorded until the maximum concentration for complete saturation of methane in the experimental fluid is reached. This procedure is repeated at each time step in the concentration vs time graph at each experimental pressure and flow rate of methane.

Calculations

For each set of experimental tests to determine the absorption mass transfer coefficient at specific conditions, several sets of data were recorded and the results are shown in Appendix Table A.1. As methane flows through the testing fluid, diesel, and internal olefin, the methane is absorbed into the fluid at various rates until complete saturation is reached. Figure 2 shows the total amount of methane (L) absorbed into the internal olefins at 100 psi and a range of superficial gas velocities. 1.6 liters of total gas was absorbed to reach complete saturation at 100 psi. Once the pressure was increased to 200 psi, the internal olefin fluid can hold twice as much dissolved methane at 3.3 liters. The amount of gas absorbed into the experimental fluid was determined from the outlet flowmeter following the flow of gas through the fluid for different amounts of time. Several tests ranging from 30 seconds to 20 minutes were conducted until complete saturation was reached at each gas velocity.

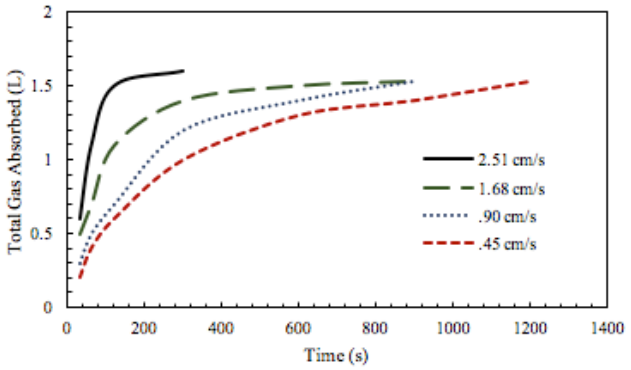

Figure 2: Total gas absorbed (L) of methane in internal olefin fluid at 100 psi and superficial gas velocities ranging from 0.45 cm/s to 2.51 cm/s

After the total amount of absorbed gas (L) is determined in Figure 2, the concentration of methane dissolved into 0.5 liters of internal olefins was calculated. Figure 3 shows that as the gas begins to flow through the pure fluid, the concentration of gas dissolved into liquid increases rapidly within the first 2 minutes at each gas velocity. At high gas velocities, complete saturation is reached within 3 minutes, while at low gas velocities it takes several minutes before saturation is reached. The difference between the maximum concentration and the concentration of gas in liquid at a specific time becomes less as complete saturation is approached. As the saturation limit is approached, the rate of absorption slows as less gas can be dissolved into the liquid at that point.

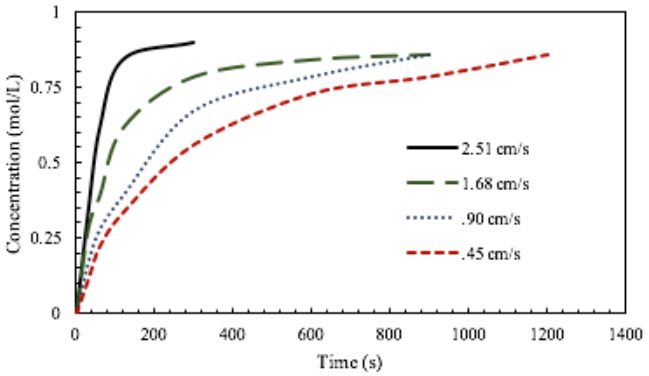

Figure 3: Concentration of gas (mol/L) dissolved into internal olefin fluid overtime at superficial gas velocities ranging from 0.45 cm/s to 2.51 cm/s

In the experimental data in Appendix Table A.1, the calculation of $\ln\left(\frac{C^*}{C^*-C_L}\right)$ at each time interval from 0.5-20 minutes for each superficial gas, velocity is shown. The concentration (C_L) at each time interval is recorded until the maximum concentration (C^*) or complete saturation is reached. In Figures 4 and 5, the absorption mass transfer coefficient can be obtained from the linear slope on the graph of $\ln\left(\frac{C^*}{C^*-C_L}\right)$ vs time. At higher superficial gas velocities, the slope of the graph of $\ln\left(\frac{C^*}{C^*-C_L}\right)$ vs time increases because complete saturation is reached in a short amount of time. As a result, k_La increases with an increase in superficial gas velocities at constant pressure.

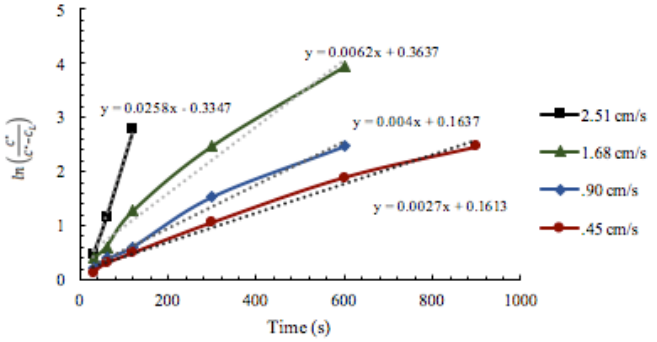

Figure 4: $\ln\left(\frac{C^*}{C^*-C_L}\right)$ vs time (s) for the calculation of k_La for methane in internal olefin fluid at 100 psi and superficial gas velocities ranging from 0.45 cm/s to 2.51 cm/s

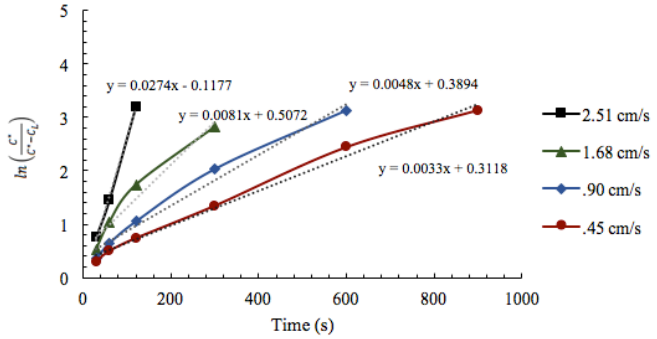

Figure 5: $\ln\left(\frac{C^*}{C^*-C_L}\right)$ vs time (s) for the calculation of k_La for methane in diesel at 100 psi and superficial gas velocities ranging from 0.45 cm/s to 2.51 cm/s

Experimental Results and Analysis

The effects of pressure and superficial gas velocity on the absorption mass transfer coefficient with H_2, CO, and CO_2 in liquid paraffin were experimentally discovered (Jin et al. 2014). The experiments were conducted at similar pressure conditions, 1.0-3.0 MPa (145 psi-435 psi), and higher superficial gas velocities, 2.5-9.0 cm/s, than the absorption experiments for methane in nonaqueous base fluids. In Figure 6, for all three gases absorbing into (liquid), the k_La value increases with increasing pressure. As the pressure is increased, higher gas density results in bubble breakup leading to a larger interfacial area between the smaller gas bubbles and the liquid during absorption processes. As the interfacial area increases at each increased pressure interval, the k_La value increases as the superficial gas velocity is held constant.

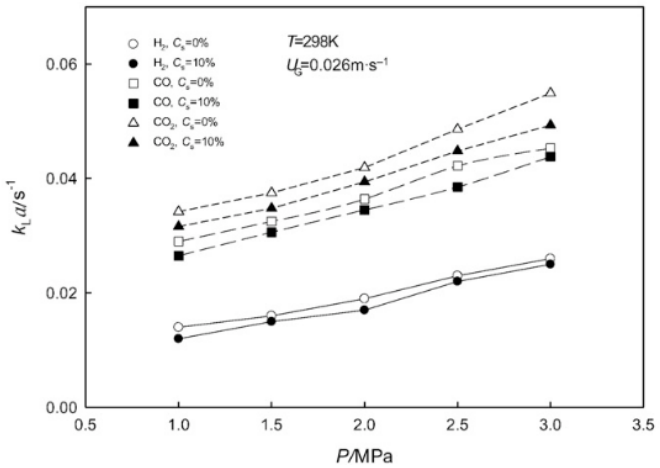

Figure 6: Influence of pressure on mass transfer coefficient (Jin et al. 2014)

The effects of gas velocity for H_2, CO, and CO_2 in liquid paraffin on the k_La value were determined by conducting experiments at a constant pressure of 1.0 MPa with gas velocities from 2.5-9.0 cm/s (Jin et al. 2014). Like the effect of increased pressure, the k_La value increases with increasing superficial gas velocity. Gas-holdup and the liquid side mass

transfer coefficient (k_L) is known to increases with gas velocity leading to an increase in gas-liquid interfacial area (Jin et al. 2014). As k_L and interfacial area increases, there is an increase in the k_La value with superficial gas velocity.

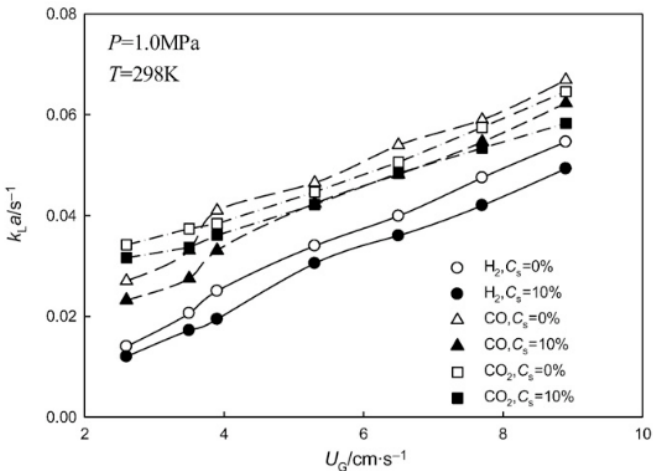

Figure 7: Influence of superficial velocity on mass transfer coefficient (Jin et al. 2014)

The effects of superficial gas velocity, system pressure and base fluid type on the k_La value were determined from the experimental test matrix. A full factorial design of 8 experimental tests was conducted and the resulting k_La values are shown in Figure 8. At constant pressures of 100 and 200 psig, the k_La value increases as the superficial gas velocity increases from 0.45 to 0.9 cm/s. Like with increasing gas velocity, the k_La value also increases with increasing system pressure as the superficial gas velocity is held constant. The effects of these 2 parameters on the absorption coefficient is the same for methane in both diesel and internal olefin fluids. For all experimental conditions, the k_La value is larger for methane in diesel than the k_La value for methane in internal olefins.

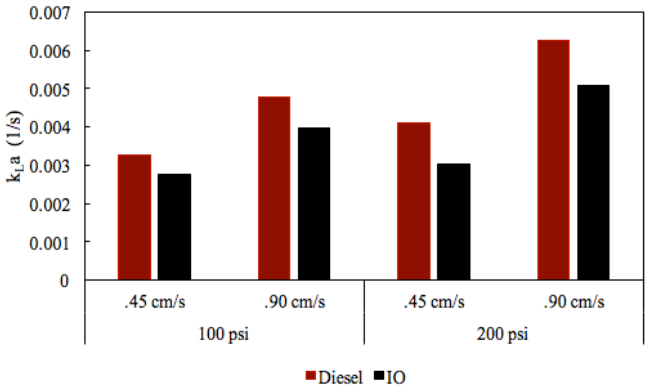

Figure 8: Effects of superficial gas velocity and system pressure on absorption coefficient for methane absorption in nonaqueous fluids

Once each parameter was investigated to determine the effect on the k_La value, a sensitivity analysis was conducted to determine which parameter has the greatest impact on the k_La. In Minitab, the full factorial design results were analyzed and Figure 9 shows that superficial gas velocity is the most important parameter affecting the k_La value. Although fluid type and pressure impact the k_La value, the superficial gas velocity has the greatest influence on the absorption coefficient. Following this parameter analysis, additional experiments were performed at 1.68 and 2.51 cm/s for both diesel and internal olefin fluids at 100 and 200 psig.

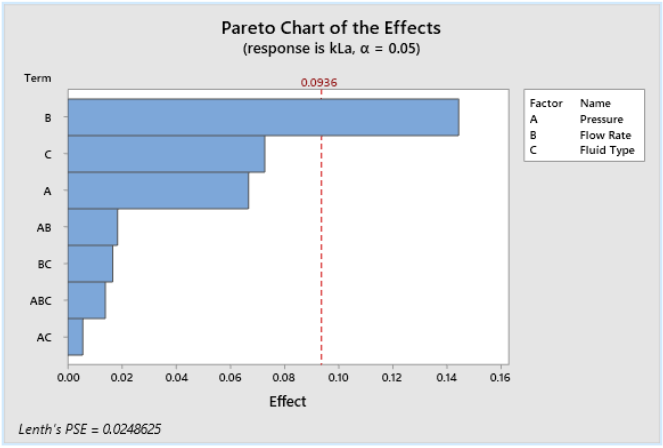

Figure 9: Minitab analysis of the full factorial design of experiments to determine parameter effects on the k_La value

After determining which paramter has the most significant impact on the k_La value, additional experimental tests were performed at higher superficial gas velocities. For both diesel and internal olefin fluids at 100 psig, tests were performed at gas velocities of 1.68 and 2.51 cm/s. The k_La value continued to increase with increasing superficial gas velocity, but it increased significantly once the velocity was increased to 2.51 cm/s. Compared to the experimental results from Jin et al. 2014, the k_La value for methane in nonaqueous fluids was in the same magnitude at similar superficial gas velocities and system pressure.

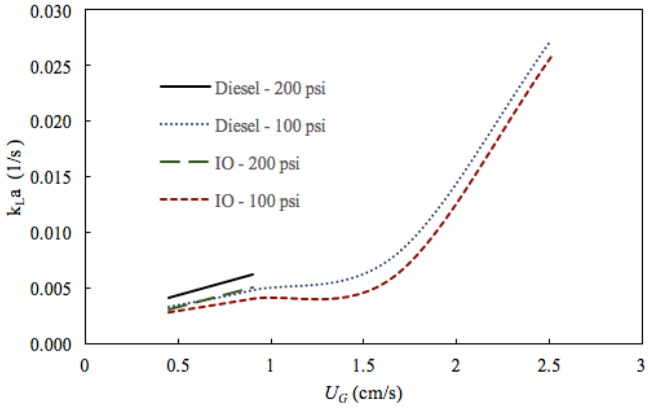

Figure 10: Influence of superficial gas velocity on the absorption coefficient for methane in nonaqueous fluids

Sensitivity Analysis of k_La for Riser Gas Handling Events

To analyze the impact of the time-dependent gas absorption into uncontaminated muds on the unloading behaviors in riser gas management events, we simulated the process of gas migration using a simplified two-phase model that is recently developed. The time-dependent gas absorption is calculated using a kinetic sub-model developed based on the experimental study in this work.

The drilling fluid in this case is assumed to be non-aqueous mud and a section of contaminated mud (containing both free and dissolved gas) has entered the riser above the SSBOP when the influx is detected. The total mass of gas influx is assumed to be 70 kg. The riser length is assumed to be 1500 m. The outer diameter of the riser annulus is 19-1/4 in, and the inner diameter is 5 in. The initial in-flow rate of gas influx is assumed as 150 scf/s. A constant temperature gradient of 20.4 - 0.025·Δh ℃ is assumed along the riser length. The gas is reservoir gas with a specific gravity of 0.65. Interfacial tension of 27 mN/m is assumed between the two phases. Mud density is 898 kg/m3 and plastic viscosity is 49 mPa·s. The time step is 0.1 s and the number of cells is 1500 for all cases to eliminate the effect of numerical dissipation. Both the entire riser and the contaminated mud section are discretized in this case.

The initial condition of the case studies are established in the way that after the influx is detected and SSBOP closed, (either with or without the assistance of mud circulation through the booster line) the main body of the gas influx has been circulated to a depth where there is a considerable slip between the gas and liquid phase, and any circulation is then ceased to allow the gas influx to migrate and expand and being absorbed into overlying uncontaminated muds while migrating under different back pressures. The contaminated mud is assumed to be saturated with gas before backpressure is applied. One dimensional flow without heat transfer between the gas and liquid phases is assumed along the riser. Sensitivity analyses are conducted in this section to study the effect of k_La on SSBOP pressure and surface flow rates with different backpressures.

Figure 11 presents the change of pressure at the subsea SSBOP level over time with different values of k_La. A backpressure of 500 psig was applied from the surface in this case. During the process of gas migration, increased values of k_La results in increased pressure-drop at the SSBOP level and a later occurrence of rapid riser unloading. In the case without gas absorption ($k_La = 0$), by the time gas influx reaches the surface, the pressure at SSBOP level dropped 1060 psi and rapid unloading occurs at approximately 55 minutes after shut-in. However, for the case of $k_La = 0.2$, BOP pressure dropped 665 psi and rapid unloading occurs at 79 minutes. This effect is observed to be even more significant when gas absorption is considered as an instantaneous process ($k_La = \infty$). Figure 11 indicates that the severity of riser unloading can be overestimated without the consideration of the time-dependent gas absorption process, and the value of the absorption coefficient, k_La, can significantly affect the riser unloading behavior.

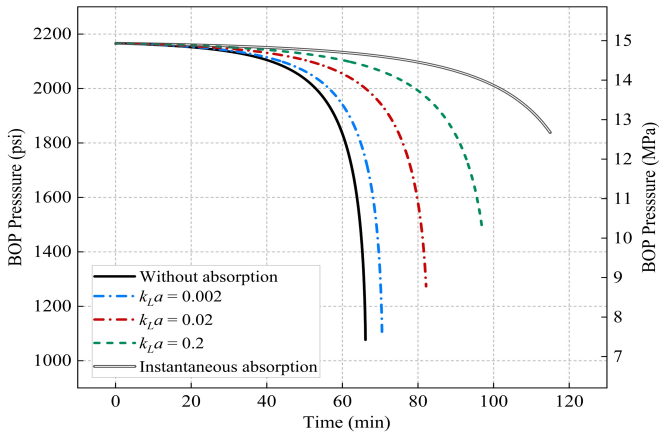

Figure 11: The Pressure at the subsea BOP level with different values of the absorption coefficient (at 500 psig / 3.45 MPa of backpressure)

Figure 12 shows the change of liquid flow rate over time at the surface level with different k_La values and at different backpressures (0 to 1000 psig). In agreement with the previous results, at the same backpressure, riser rapid unloading occurs later and the maximum liquid flow rate at the surface decreases when k_La value increases. The application of backpressure can effectively delay the occurrence of the rapid riser unloading and decrease the maximum liquid velocities in all cases with different k_La values. However, the effect of gas absorption is observed to be more significant under higher backpressures. For the case of $k_La = 0.2$, the maximum velocity at the surface is predicted to be 17.2 m/s with no backpressure, while the maximum surface velocity is 7.1 m/s at the backpressure of 1000 psig. Such decrease is not as apparent when gas absorption is not considered. For the case of instantaneous absorption ($k_La = \infty$), at a backpressure of 1000 psig, gas influx can maintain near completely dissolved until the contaminated mud section reaches the surface.

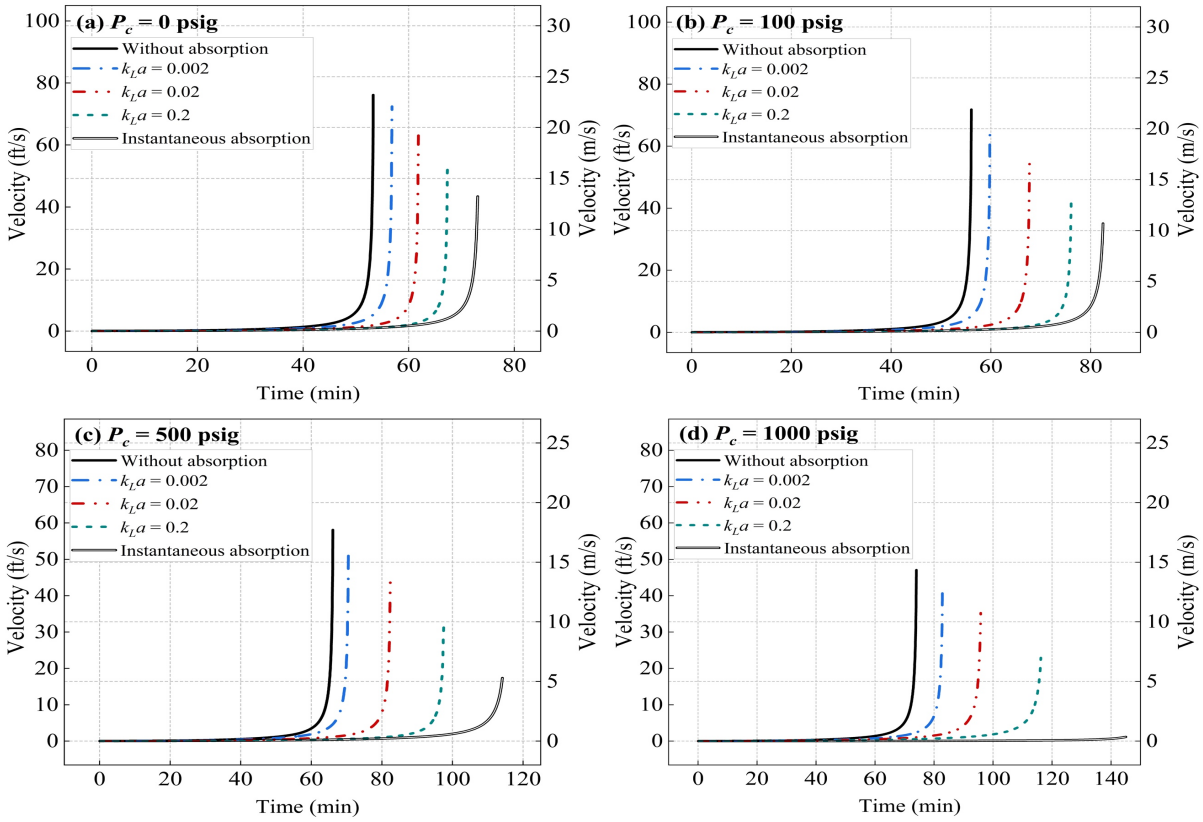

Figure 12— The liquid flow rate at the surface with different values of the absorption coefficient (at backpressures of (a) 0 psig, (b) 100 psig, (c) 500 psig, and (d) 1000 psig)

Conclusions

The absorption mass transfer coefficient was experimentally investigated in a bubble column to determine the k_La value for methane gas in nonaqueous base fluids at high-pressure conditions. The study analyzes the effect of system pressure up to 200 psi and superficial gas velocities between 0.45 and 2.51 cm/s on the mass transfer coefficient. Two commonly used nonaqueous base fluids in drilling processes, diesel and internal olefins, were used in the experimental study to better understand the mass transfer of a gas influx in oil base fluids. All three parameters had a significant impact on k_L, as the absorption coefficient increased with increased superficial gas velocity, increased system pressure, and the resulting k_La value was higher for diesel than internal olefins. An increased understanding of absorption mass transfer and k_La between methane and nonaqueous drilling fluids can lead to early detection of gas influxes and to optimize well control in such events.

Sensitivity analyses based on numerical simulations were conducted to study the effect of k_La on the gas migration behaviors at different backpressures. Results show that the severity of riser unloading was overestimated without out the consideration gas desorption, and the value of the absorption coefficient can significantly affect the riser unloading behavior. Increased values of k_La results in increased pressure-drop at the SSBOP level and lower maximum liquid velocities at the surface. The impact of time-dependent gas absorption process on riser unloading is more significant at higher backpressures.

Acknowledgments

This work is supported by the NAS Gulf Research Program, Louisiana Board of Regents (Grant contract number LEQSF(2019-22)-RD-B-02), Blade Energy Partners, and Louisiana State University Craft & Hawkins Department of Petroleum Engineering. The authors would also like to thank Halliburton for the donation of the synthetic fluids used for experiments in this study.

Nomenclature

C^*	=	Maximum gas concentration [mol/L]
C_i	=	Initial concentration of gas in liquid [mol/L]
C_L	=	Concentration of gas in liquid [mol/L]
C_f	=	Final concentration of gas in liquid [mol/L]
d_B	=	Bubble diameter [m]
D	=	Column diameter [cm]
D_L	=	Diffusivity of solute gas into liquid [m^2/s]
g	=	Acceleration due to gravity [m/s^2]

$k_L a$ = Volumetric mass-transfer coefficient [1/s]
t = Time [s]
U_l = Liquid velocity [cm/s]
U_G = Superficial gas velocity [cm/s]

Greek Letters

γ = Surface Tension [M/T^2]
ϵ_G = Gas holdup
μ_l = Liquid viscosity [Pa*s]
ρ_G = Gas density [kg/m^3]
ρ_L = Liquid density [kg/m^3]
σ = Liquid surface tension [dyn/cm]

References

1. Akita, Kiyomi, and Fumitake Yoshida. 1973. "Gas Holdup and Volumetric Mass Transfer Coefficient in Bubble Columns. Effects of Liquid Properties." Industrial & Engineering Chemistry Process Design and Development12, no. 1 (1973): 76–80. https://doi.org/10.1021/i260045a015.
2. Al-Areeq, Nabil Mohammed. 2018. "Petroleum Source Rocks Characterization and Hydrocarbon Generation." Recent Insights in Petroleum Science and Engineering, July 2018. https://doi.org/10.5772/intechopen.70092.
3. Álvarez, E., B. Sanjurjo, A. Cancela, and J.m. Navaza. 2000. "Mass Transfer and Influence of Physical Properties of Solutions in a Bubble Column." Chemical Engineering Research and Design78, no. 6 (2000): 889–93. https://doi.org/10.1205/026387600527950.
4. Elhajj, Jessy, Mahmoud Al-Hindi, and Fouad Azizi. 2013. "A Review of the Absorption and Desorption Processes of Carbon Dioxide in Water Systems." *Industrial & Engineering Chemistry Research*53, no. 1 (2013): 2–22. https://doi.org/10.1021/ie403245p.
5. Gandhi, Ankit B., Prashant P. Gupta, Jyeshtharaj B. Joshi, Valadi K. Jayaraman, and Bhaskar D. Kulkarni. 2009. "Development of Unified Correlations for Volumetric Mass-Transfer Coefficient and Effective Interfacial Area in Bubble Column Reactors for Various Gas−Liquid Systems Using Support Vector Regression." *Industrial & Engineering Chemistry Research*48, no. 9 (June 2009): 4216–36. https://doi.org/10.1021/ie8003489.
6. Jin, Haibo, Suohe Yang, Guangxiang He, Delin Liu, Zemin Tong, and Jianhua Zhu. 2014. "Gas–Liquid Mass Transfer Characteristics in a Gas–Liquid–Solid Bubble Column under Elevated Pressure and Temperature." Chinese Journal of Chemical Engineering22, no. 9 (2014): 955–61. https://doi.org/10.1016/j.cjche.2014.06.019.
7. Lau, R., W. Peng, L. G. Velazquez-Vargas, G. Q. Yang, and L.-S. Fan. 2004. "Gas−Liquid Mass Transfer in High-Pressure Bubble Columns." Industrial & Engineering Chemistry Research43, no. 5 (2004): 1302–11. https://doi.org/10.1021/ie030416w.
8. Malloy, Kenneth P., Rick Stone, George Harold Medley, Don M. Hannegan, Oliver D. Coker, Don Reitsma, Helio Mauricio Santos, et al. 2009. "Managed-Pressure Drilling: What It Is and What It Is Not." IADC/SPE Managed Pressure Drilling and Underbalanced Operations Conference & Exhibition, 2009. https://doi.org/10.2118/122281-ms.
9. Neff, Jerry M., S. McKelvie, and R. C. Ayers. 2000. Environmental Impacts of Synthetic Based Drilling Fluids. New Orleans: U.S. Dept. of the Interior, Minerals Management Service, Gulf of Mexico OCS Region, 2000.
10. O'bryan, Patrick Leon. 1983. "The Experimental and Theoretical Study of Methane Solubility in an Oil-Base Drilling Fluid.". LSU Historical Dissertations and Theses. 1983.
11. Öztürk, S. S., A. Schumpe, and W.-D. Deckwer. 1987. "Organic Liquids in a Bubble Column: Holdups and Mass Transfer Coefficients." AIChE Journal33, no. 9 (1987): 1473–80. https://doi.org/10.1002/aic.690330907.
12. Selley, Richard C., and Stephen A. Sonnenberg. 2016. Elements of Petroleum Geology. Amsterdam: Academic Press, 2016.
13. Wilkinson, Peter M., Herman Haringa, and Laurent L. Van Dierendonck. 1994. "Mass Transfer and Bubble Size in a Bubble Column under Pressure." Chemical Engineering Science49, no. 9 (1994): 1417–27. https://doi.org/10.1016/0009-2509(93)e0022-5.

Appendix A

Table A.1: Experimental data used to calculate the $k_L a$ value

Test	*Flow Rate (ln/min)*	*Time (min)*	*Total Absorbed (L)*	*n (mol)*	*Concentration (mol/L)*	$ln\left(\frac{C^*}{C^* - C_L}\right)$
1	1	0.5	0.2	0.056191086	0.112382171	0.140088793
2	1	1	0.4	0.112382171	0.224764343	0.303050103
3	1	2	0.6	0.168573257	0.337146514	0.497838428
4	1	5	1	0.280955428	0.561910857	1.060146008
5	1	10	1.3	0.365242057	0.730484114	1.894943705
6	1	15	1.4	0.3933376	0.7866752	2.465488564
7	1	20	1.53	0.429861806	0.859723611	

Test	*Flow Rate (ln/min)*	*Time (min)*	*Total Absorbed (L)*	*n (mol)*	*Concentration (mol/L)*	$ln\left(\frac{C^*}{C^* - C_L}\right)$
1	2	0.5	0.3	0.084286629	0.168573257	0.218253566
2	2	1	0.5	0.140477714	0.280955428	0.395708933
3	2	2	0.7	0.1966688	0.3933376	0.611597314
4	2	5	1.2	0.337146514	0.674293028	1.53393036
5	2	10	1.4	0.3933376	0.7866752	2.465488564
6	2	15	1.53	0.429861806	0.859723611	

Test	*Flow Rate (ln/min)*	*Time (min)*	*Total Absorbed (L)*	*n (mol)*	*Concentration (mol/L)*	$ln\left(\frac{C^*}{C^* - C_L}\right)$
1	4	0.5	0.5	0.140477714	0.280955428	0.395708933
2	4	1	0.7	0.1966688	0.3933376	0.611597314
3	4	2	1.1	0.309050971	0.618101943	1.269237806
4	4	5	1.4	0.3933376	0.7866752	2.465488564
5	4	10	1.5	0.421433143	0.842866285	3.931825633
6	4	15	1.53	0.429861806	0.859723611	

Test	*Flow Rate (ln/min)*	*Time (min)*	*Total Absorbed (L)*	*n (mol)*	*Concentration (mol/L)*	$ln\left(\frac{C^*}{C^* - C_L}\right)$
1	6	0.5	0.6	0.168573257	0.337146514	0.470003629
2	6	1	1.1	0.309050971	0.618101943	1.16315081
3	6	2	1.5	0.421433143	0.842866285	2.772588722
4	6	5	1.6	0.449528686	0.899057371	